

Application of nanofluids for heat transfer enhancement of separated flows encountered in a backward facing step

Eiyad Abu-Nada *

Department of Mechanical Engineering, Hashemite University, Zarqa 13115, Jordan

Received 29 March 2007; received in revised form 19 June 2007; accepted 1 July 2007

Available online 20 August 2007

Abstract

Numerical investigation of heat transfer over a backward facing step (BFS), using nanofluids is presented. Different volume fractions of nanoparticles are presented in the base fluid besides different type of nanoparticles have been used. The finite volume technique is used to solve the momentum and energy equations. The distribution of Nusselt number at the top and the bottom walls of the BFS are obtained. For the case of Cu nanoparticles, there was an enhancement in Nusselt number at the top and bottom walls except in the primary and secondary recirculation zones where insignificant enhancement is registered. It was found that outside the recirculation zones, nanoparticles having high thermal conductivity (such as Ag or Cu) have more enhancements on the Nusselt number. However, within recirculation zones, nanoparticles having low thermal conductivity (such as TiO_2) have better enhancement on heat transfer. An increase in average Nusselt number with the volume fraction of nanoparticles for the whole range of Reynolds number is registered.

© 2007 Elsevier Inc. All rights reserved.

Keywords: Nanofluids; Separated flows; Heat transfer; Backward facing step

1. Introduction

Heat transfer in separated flows is frequently encountered in various engineering applications. Some examples include combustors, heat exchangers, axial and centrifugal compressor blades, gas turbines blades, and microelectronic circuit boards. It is well known that heat transfer characteristics experience large variation within separated regions. Thus, it is very essential to understand the mechanisms of heat transfer in such regions in order to enhance heat transfer. An innovative technique for improving heat transfer by using ultra fine solid particles in the fluids has been used extensively during the last decade. The term nanofluid refers to these kinds of fluids by suspending nano-scale particles in the base fluid (Choi, 1995). The particles are different from conventional particles (millimeter or micro-scale) in that they keep suspended in the fluid

and no sedimentation occurs which causes no increase in pressure drop in the flow field (Daungthongsuk and Wongwises, 2007). Therefore, it is very useful to enhance heat transfer in separated regions by using nanofluids. Such enhancement is accomplished by increasing the value of convective heat transfer coefficient (or Nusselt number) in separated flows.

The past decade has witnessed extensive research on the convective heat transfer in nanofluids. Recently, Trisaksri and Wongwises (2007) conducted a literature review on the general heat transfer characteristics of nanofluids. Moreover, Daungthongsuk and Wongwises (2007) performed a comprehensive review on convective heat transfer in nanofluids. Additionally, Wang and Mujumdar (2007) conducted a review on heat transfer characteristics in nanofluids. The literature search indicates that the application of nanofluids on the heat transfer enhancement of separated flows has not been investigated yet. The flow over a backward facing step (BFS) has the most basic features of separated flows, such as separation, reattachment,

* Tel.: +962 390 3333; fax: +962 382 6613.

E-mail address: eyad@hu.edu.jo

Nomenclature

a	upstream channel height (m)	x_1	beginning of the secondary recirculation bubble, dimensionless
c_p	specific heat at constant pressure ($\text{kJ kg}^{-1} \text{K}^{-1}$)	x_2	end of the secondary recirculation bubble, dimensionless
D_H	hydraulic diameter at inlet ($D_H = 2a$) (m)	x_r	reattachment length, dimensionless
ER	expansion ratio (H/S), dimensionless	y^*	dimensionless vertical coordinate
h	convection heat transfer coefficient ($\text{W m}^{-2} \text{K}^{-1}$)	y	vertical distance (m)
H	downstream channel height (m)		
k	thermal conductivity ($\text{W m}^{-1} \text{K}^{-1}$)		
L	length of the channel (m)		
M	number of grid points in horizontal direction		
N	number of grid points in vertical direction		
Nu	Nusselt number ($\frac{h(D_H)}{k}$)		
Nu_{avg}	average Nusselt number		
p^*	dimensionless pressure		
p	pressure (N m^{-2})		
Pr	Prandtl number		
q_w	heat flux at the wall (W m^{-2})		
Re	Reynolds number ($\frac{u_m D_H}{v}$)		
S	step height (m)		
T	dimensional temperature (K)		
u_m	average velocity of the incoming flow at inlet (m/s)		
u	dimensionless x component of velocity		
u^*	x component of velocity (m/s)		
v	dimensionless y component of velocity		
v^*	y component of velocity (m/s)		
x	dimensionless horizontal coordinate		
x^*	horizontal distance (m)		

Greek symbols

α	thermal diffusivity (m^2/s)
ε	numerical tolerance
ϕ	transport quantity
ϕ	nanoparticle volume fraction
μ	dynamic viscosity (Ns m^{-2})
θ	dimensionless temperature
ρ	density

Subscripts

avg	average value
b	bulk value
nf	nanofluid
f	fluid
resid	residual
s	solid
w	wall
wc	cold wall
wh	hot wall
∞	far-stream

recirculation, and development of shear layers. Therefore, it is very useful to study the effect of nanofluids on the BFS to characterize the enhancement of heat transfer in separated flows.

The problem of fluid flow over a backward facing step has been studied extensively in the last three decades (Armany et al., 1983; Kim and Moin, 1985; Thangam and Knight, 1989; Gartling, 1990; Williams and Baker, 1997; Li and Armany, 2002; Tylli et al., 2002; Nie and Armany, 2003; Abu-Nada et al., 2007). Abu-Mulaweh (2003) conducted an extensive review of research on laminar mixed convection over a BFS.

The extensive interest and research conducted on BFS, in the last two decades, with the complex physics encountered in separated flow over the BFS and the continuous interest in nanofluids has motivated the present investigation. Therefore, the goal of this research is to study heat transfer characteristics of flow over a backward facing step using nanofluids. The problem is investigated numerically by solving the Navier-Stokes and energy equations (NSE). Heat transfer characteristics are analyzed for a wide range of volume fractions of the nanoparticles, Reynolds numbers and various types of nanofluids.

2. Problem description and governing equations

The basic flow configuration, under study, is shown in Fig. 1. The expansion ratio (ER = H/S) is set equal to 2.0. The flow is assumed Newtonian, two-dimensional, steady and incompressible. It is assumed that the base fluid (i.e. water) and the nanoparticles are in thermal equilibrium and no slip occurs between them. Thermophysical

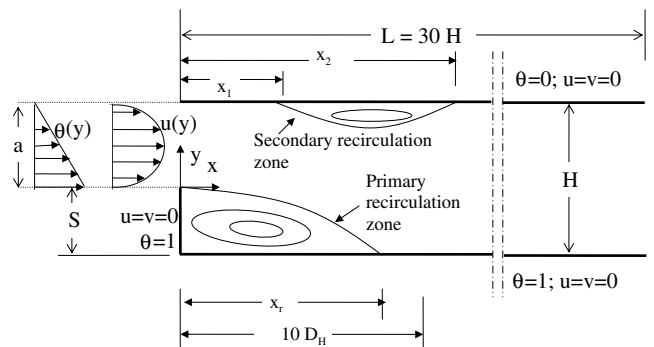


Fig. 1. Sketch of the problem geometry and boundary conditions.

Table 1
Thermophysical properties

Property	Fluid phase (Water)	Cu	Ag	CuO	Al ₂ O ₃	TiO ₂
c_p (J/kg K)	4179	385	235	535.6	765	686.2
ρ (kg/m ³)	997.1	8933	10500	6500	3970	4250
k (W/m K)	0.613	400	429	20	40	8.9538
$\alpha \times 10^7$ (m ² /s)	1.47	1163.1	1738.6	57.45	131.7	30.7

properties of the nanofluid are given in Table 1. In current formulation, thermophysical properties of the nanofluid are assumed to be constant.

Introducing the following dimensionless quantities:

$$x = \frac{\hat{x}}{D_H}, \quad y = \frac{\hat{y}}{D_H}, \quad u = \frac{\hat{u}}{u_m}, \quad v = \frac{\hat{v}}{u_m},$$

$$p = \frac{\hat{p}}{\rho u_m^2}, \quad \text{and } \theta = \frac{T - T_{wc}}{T_{wh} - T_{wc}}.$$

Then, the continuity, momentum, and energy equations, in non-dimensional form, in Cartesian coordinates are given as:

$$\frac{\partial u}{\partial x} + \frac{\partial v}{\partial y} = 0 \quad (1)$$

$$u \frac{\partial u}{\partial x} + v \frac{\partial u}{\partial y} = - \frac{1}{(1 - \varphi) + \varphi \frac{\rho_s}{\rho_f}} \frac{\partial p}{\partial x} + \frac{1}{Re} \frac{1}{\left((1 - \varphi)^{2.5} \left((1 - \varphi) + \varphi \frac{\rho_s}{\rho_f} \right) \right)} \left(\frac{\partial^2 u}{\partial x^2} + \frac{\partial^2 u}{\partial y^2} \right) \quad (2)$$

$$u \frac{\partial v}{\partial x} + v \frac{\partial v}{\partial y} = - \frac{1}{(1 - \varphi) + \varphi \frac{\rho_s}{\rho_f}} \frac{\partial p}{\partial y} + \frac{1}{Re} \frac{1}{\left((1 - \varphi)^{2.5} \left((1 - \varphi) + \varphi \frac{\rho_s}{\rho_f} \right) \right)} \left(\frac{\partial^2 v}{\partial x^2} + \frac{\partial^2 v}{\partial y^2} \right) \quad (3)$$

$$u \frac{\partial \theta}{\partial x} + v \frac{\partial \theta}{\partial y} = \frac{1}{Re Pr} \left(\frac{\frac{k_{nf}}{k_f}}{(1 - \varphi) + \varphi \frac{(pc_p)_s}{(pc_p)_f}} \right) \left(\frac{\partial^2 \theta}{\partial x^2} + \frac{\partial^2 \theta}{\partial y^2} \right) \quad (4)$$

where

$$Re = \frac{\rho_f u_m D_H}{\mu_f},$$

$$Pr = \frac{\nu_f}{\alpha_f}.$$

In Eqs. (1)–(4), the viscosity of the nanofluid is approximated as viscosity of a base fluid μ_f containing dilute suspension of fine spherical particles and is given by (Brinkman, 1952):

$$\mu_{nf} = \frac{\mu_f}{(1 - \varphi)^{2.5}} \quad (5)$$

The effective density of the fluid is given as

$$\rho_{nf} = (1 - \varphi)\rho_f + \varphi\rho_s \quad (6)$$

The heat capacitance of the nanofluid is expressed as (Khanafer et al., 2003):

$$(\rho c_p)_{nf} = (1 - \varphi)(\rho c_p)_f + \varphi(\rho c_p)_s \quad (7)$$

The effective thermal conductivity of the nanofluid can be approximated by the Maxwell-Garnetts (MG) model as (Khanafer et al., 2003):

$$k_{nf} = \frac{k_s + 2k_f - 2\varphi(k_f - k_s)}{k_s + 2k_f + \varphi(k_f - k_s)} \quad (8)$$

The MG model is only restricted to spherical nanoparticles and does not take into account the shape of nanoparticles. It should be emphasized that macroscopic modeling of nanofluids is restricted to spherical nanoparticles and suitable for small temperature gradients (Shukla and Dhir, 2005). Therefore, the present formulation is limited to nanoparticles with a spherical shape.

The boundary conditions are prescribed as follows:

At the channel inlet: $u(y) = 12(y - 2y^2)$ and $\theta = 1 - 2y$.

At the channel outlet: $\frac{\partial u}{\partial x} = \frac{\partial v}{\partial x} = 0$ and $\frac{\partial \theta}{\partial x} = 0$.

The boundary conditions at the top, bottom, and step walls are shown in Fig. 1. The total length of the computational domain is taken as ($L = 30$ H) to ensure fully developed outlet boundary condition (Gartling, 1990; Vratis et al., 1992; Pepper et al., 1992; Abu-Nada, 2006; Abu-Nada et al., 2007).

3. Numerical Implementation

Eqs. (1)–(4), with corresponding boundary conditions are solved using the finite volume approach. The SIMPLE algorithm is used as the computational algorithm (Patankar, 1980; Versteeg and Malalasekera, 1995). The diffusion term in the momentum and energy equations is approximated by second-order central difference which gives a stable solution. Furthermore, a second-order upwind differencing scheme is adopted for the convective terms.

In the x direction, a fine grid is used in the regions near the point of reattachment to resolve the steep velocity gradients while a coarser grid is used downstream of that point (Anderson, 1995). However, in the y direction, a fine grid is used near the top, the bottom walls, and directly at the step. A fine mesh in the x and y directions is generated by using an algebraic grid stretching technique that results in considerable savings in terms of the grid size and computational time. For more details on grid stretching implementation, the readers are referred to Abu-Nada et al. (2007).

The algebraic finite volume equations for the momentum and energy equations are solved using the tri-diagonal matrix algorithm (Thomas algorithm) with the line-by-line relaxation technique. The convergence criteria were defined by the following expression:

$$\varepsilon = \frac{\sum_{j=1}^{j=M} \sum_{i=1}^{i=N} |\text{resid}_{ij}|}{\sum_{j=1}^{j=M} \sum_{i=1}^{i=N} |\phi_{ij}|} < 10^{-5}, \quad (9)$$

The symbol ϕ holds for u , v , or T and ε is the tolerance and resid is the residual; M and N are the number of grid points in the x and the y directions, respectively.

After solving for u , v , and T , further useful quantities are obtained. For example, the Nusselt number on the bottom wall is written as:

$$Nu = -\frac{1}{(\theta_w - \theta_b)} \frac{k_{nf}}{k_f} \left. \frac{\partial \theta}{\partial y} \right|_{y=-1/2} \quad (10)$$

where θ_b is bulk temperature. Similar expression could be written for the top wall. The average Nusselt number is defined as:

$$Nu_{\text{avg}} = \frac{\int_0^L \sqrt{(Nu(x))^2} dx}{L} \quad (11)$$

4. Grid testing and code validation

Extensive mesh testing was performed to guarantee a grid independent solution. The problem selected for the grid testing is the flow over a BFS using air as the working fluid. A grid size of 125×250 (125 grid points in y and 250 grid points in x) ensures a grid independent solution. Also, a grid independence test is carried out for the nanofluid case for $\phi = 0.2$ and $Re = 600$. The grid independence test for the nanofluid case shows that a grid size of 125×250 ensures a grid independent solution. The present results are carried out on a grid size of 151×299 .

The present numerical solution is validated by comparing the present code results for the benchmark problem for $Re = 800$, $Pr = 0.7$, and $ER = 2.0$ with the experiment of Armaly et al. (1983) and with other numerical published data. As shown in Fig. 2, the code results are very close to the previous numerical published results. However, all of the numerical published works, including the present one, underestimate the reattachment length. According to Armaly et al. [1], the flow at $Re = 800$ has three-dimensional features. Therefore, the underestimation of x_r , by all numerical published data is due to the two-dimensional assumption embedded in the numerical solution (Armaly

et al., 1983; Thangam and Knight, 1989). More specifically, it is due to the side wall induced three-dimensional effects (Williams and Baker, 1997; Tylly et al., 2002). To avoid three-dimensionality of the flow, the results are restricted to $Re \leq 600$.

5. Results and discussion

The range of Reynolds number used in the present research is $200 \leq Re \leq 600$ and the range of nanoparticles volume fraction is $0 \leq \phi \leq 0.2$. The Prandtl number of the base fluid (water) is kept constant at 6.2. Five different types of nanoparticles are studied which are Cu, Ag, Al_2O_3 , CuO , and TiO_2 .

Fig. 3a shows the distribution of the Nusselt number at the top wall for $Re = 200$ using different nanoparticles volume fractions. The figure reveals an enhancement in Nusselt number by increasing the volume fraction of nanoparticles. This behavior is explained by looking at Eq. (10). The expression of the Nusselt number consists of three terms which are the term for the temperature difference between the wall and the fluid bulk temperature (i.e. $1/(\theta_w - \theta_b)$), the term for thermal conductivity ratio (i.e. k_{nf}/k_f), and the term for the temperature gradient at the wall (i.e. $d\theta/dy$). To illustrate the effect of volume fraction of nanoparticles on these terms, Fig. 4 is prepared. The effect of nanoparticles on the temperature difference term is negligible. However, Fig. 4a and b shows that the effect of volume fraction of nanoparticles on the temperature gradient term and on the thermal conductivity ratio term is more pronounced. Fig. 4a shows that, before the point of reattachment (See Fig. 5), as the percentage of nanoparticles increases the temperature gradient at the top wall increases. This is related to the increase in inertia forces as depicted by Eqs. (2) and (3). The equations show that inertia forces are amplified by the factor $(1 - \phi)^{2.5}[(1 - \phi) + \phi \rho_s/\rho_f]$. Therefore, any increase in volume fraction increases inertia forces and accordingly increases the temperature gradient. Besides, the nanoparticles increase the thermal conductivity ratio term as shown in Fig. 4c. Therefore, both the temperature gradient term and thermal conductivity ratio term increase by increasing the volume fraction of nanoparticles. Accordingly, the overall effect at the top wall is an enhancement in the Nusselt number by increasing the volume fraction of the nanoparticles.

The effect of volume fraction of nanoparticles on the Nusselt number at the bottom wall is shown in Fig. 3b. By comparing Figs. 3b and 5 it is clear that the maximum value of Nusselt number, on the bottom wall, coincide with the point of reattachment. After the point of reattachment, an increase in Nusselt number is observed by increasing the volume fraction of the nanoparticles. The explanation after the point of reattachment is similar to the justification presented at the top wall. However, inside the primary recirculation zone a different behavior is identified, where the Nusselt number becomes less sensitive to the presence of nanoparticles. To explain what is happening inside the

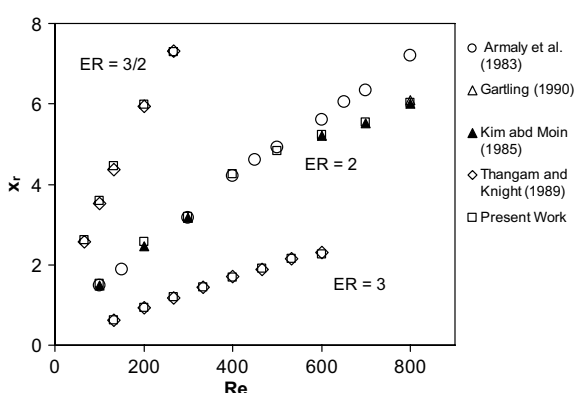


Fig. 2. Model Validation: Reattachment length versus Reynolds number for various expansion ratios, $Pr = 0.70$, $Re = 800$.

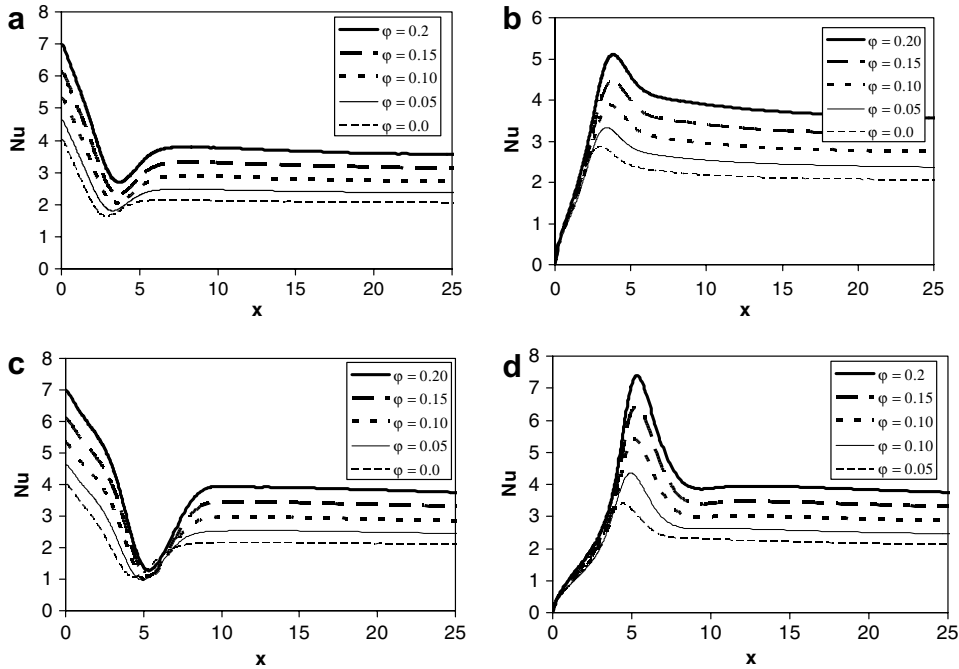


Fig. 3. Nusselt number distribution using Cu nanoparticles (a) Top wall $Re = 200$ (b) Bottom wall $Re = 200$ (c) Top wall $Re = 400$ (d) Bottom wall $Re = 400$.

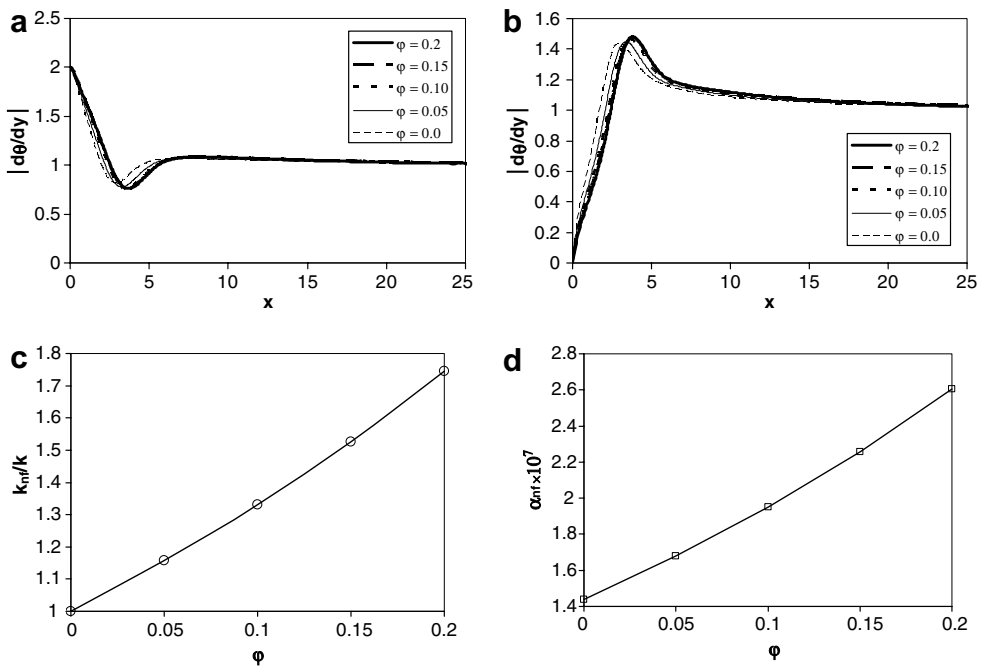


Fig. 4. (a) Temperature gradient at the top wall. (b) Temperature gradient at the bottom wall. (c) Thermal conductivity ratio versus volume fraction of nanoparticles. (d) Thermal diffusivity versus volume fraction of nanoparticles.

recirculation zone we need to look at Fig. 4 again. Fig. 4b shows that as the percentage of nanoparticles increases the temperature gradient term decreases. In fact, inertia forces within the primary recirculation zone are relatively weak and the effect of nanoparticles on increasing the inertia effect is negligible. Therefore, higher value of effective ther-

mal conductivity due to the presence of nanoparticles is the main reason for the reduction in temperature gradient at the bottom wall. In fact higher values of thermal conductivity are accompanied by higher values of thermal diffusivity, as shown in Fig. 4d. The high values of thermal diffusivity cause a drop in the temperature gradients. By

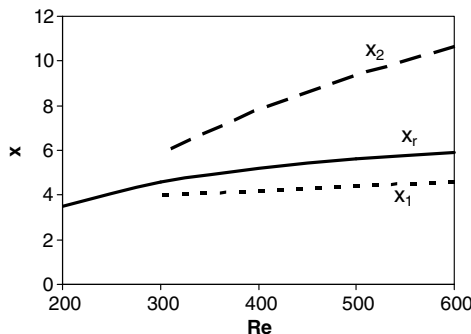


Fig. 5. Reattachment length and the beginning and the end of the upper recirculation zone versus Reynolds number using Cu nanoparticles, $\varphi = 0.20$, $Pr = 6.2$.

looking at Fig. 4b and c it is clear that the percentage of increase in thermal conductivity ratio is approximately equal to the decrease in temperature gradient. Therefore, according to Eq. (10), the multiplication of the temperature gradient term and the thermal conductivity ratio term does not affect the Nusselt number. Accordingly, the Nusselt number becomes less dependent of the volume fraction of the nanoparticles. Consequently, the high Nusselt number inside the recirculation depends mainly on the thermophysical properties of the nanoparticles and is independent of Reynolds number because of the small values of the inertia forces. However, outside the recirculation zone both the Reynolds number and the thermophysical properties of the nanofluids affect the value of Nusselt number. The optimum nanoparticle selection for the recirculation regions is nanoparticles with low thermal diffusivity. This could be done by using particles with high values of density and thermal capacitance.

Fig. 3c shows the effect of volume fraction on the Nusselt number at the top wall for $Re = 400$. For $Re = 400$, the upper secondary recirculation zone appears as shown in Figs. 5 and 6. Therefore, the behavior inside the secondary recirculation zone is similar to the behavior encountered in the primary recirculation zone, for the case of $Re = 200$. Figs. 5 and 6 show the increased size of upper secondary recirculation zone with the volume fraction of nanoparticles for $Re = 400$. Fig. 3d shows that, at the bottom wall and outside the recirculation zone, the behavior of $Re = 400$ is similar to the behavior of $Re = 200$ where an increase in the Nusselt number is observed by increasing the volume fraction of nanoparticles. It is worth mentioning that the case of $Re = 600$ has a similar trend to that of $Re = 400$. It is clear that for ($x > 10$), Nusselt number is independent of Reynolds number and is only a function of volume fraction of nanoparticles. However, around the point of reattachment the Nusselt number is a function of Reynolds number and the volume fraction of the nanoparticles.

An interesting comparison between various nanofluids is presented in Fig. 7. It is interesting to note that on the top wall, and before the beginning of the top secondary recirculation zone, nanoparticles with high thermal conductivity have more enhancements on the value of the Nusselt number. However, within the recirculation zone, nanoparticles with low thermal conductivity display more enhancements on heat transfer. This conclusion is consistent with our earlier discussion that inside the recirculation zone the fluid needs to have lower thermal diffusivity. Therefore, nanoparticles of low thermal conductivity (or low thermal diffusivity as shown in Table 1) are more appropriate for the recirculation zone. However, outside the recirculation zone

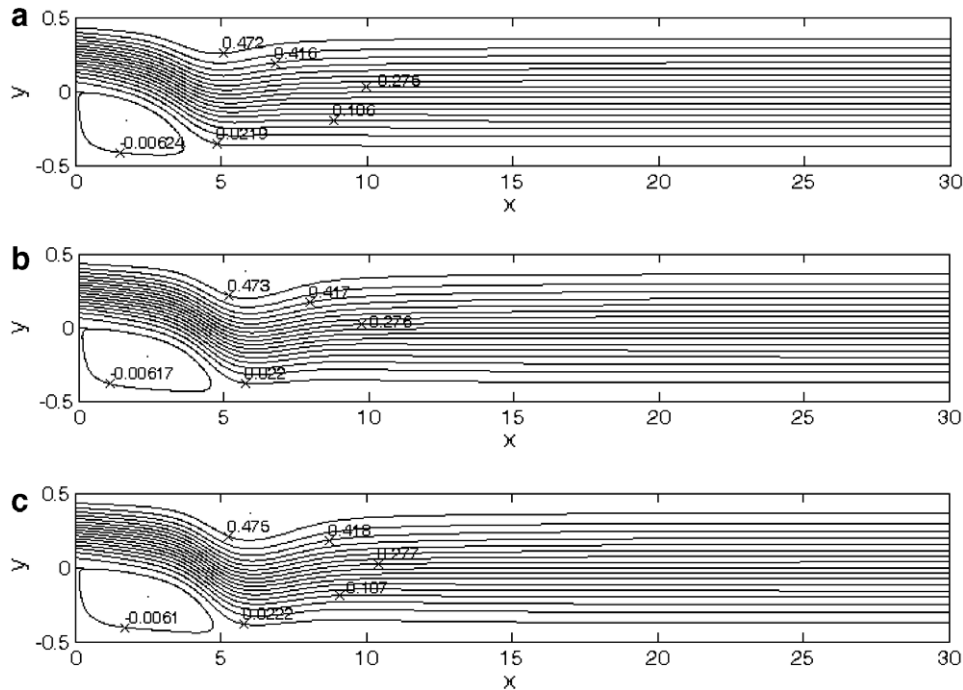


Fig. 6. Streamline patterns for Cu nanoparticles, $Re = 400$ (a) $\varphi = 0$, (b) $\varphi = 0.1$ and (c) $\varphi = 0.2$.

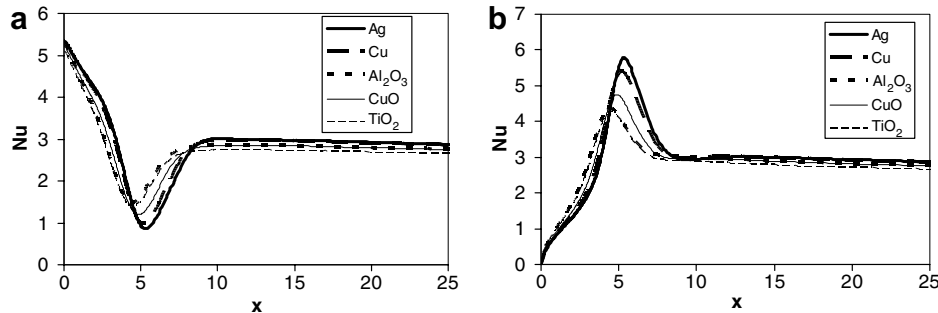


Fig. 7. Nusselt number distribution using different types of nanoparticles, $Re = 400$, $\varphi = 0.1$. (a) Top wall and (b) Bottom wall.

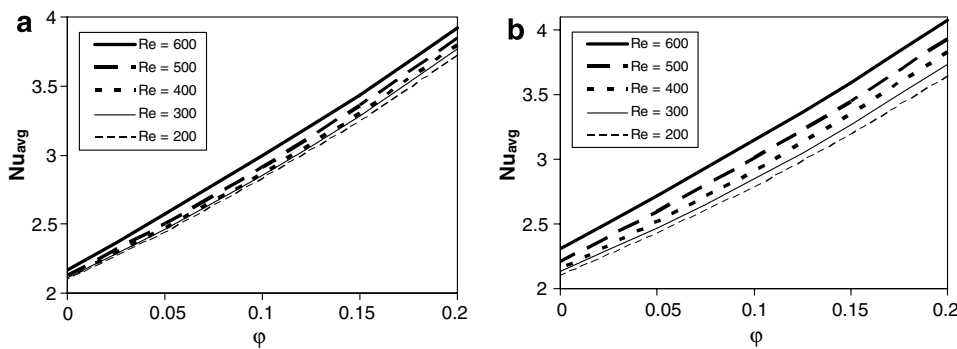


Fig. 8. Average number versus volume fraction using Cu nanoparticles. (a) Top wall and (b) Bottom wall.

nanoparticles of high thermal conductivity are more suitable.

Fig. 8 shows the average Nusselt number at the top and the bottom walls. There is an increase in the average Nusselt number with the volume fraction of nanoparticles for the whole range of Reynolds number. Also, the figure shows that the average Nusselt number is more sensitive to volume fraction than to Reynolds number.

6. Conclusions

At the top wall, and for $Re = 200$, an enhancement in the Nusselt number is registered by increasing the volume fraction of the nanoparticles. For $Re > 300$, there was an enhancement in Nusselt number at the top wall except in the secondary recirculation zone where insignificant enhancement is registered. It is found that the high Nusselt number inside the recirculation zone depends mainly on the thermophysical properties of the nanoparticles and is independent of Reynolds number. However, outside the recirculation zone both the Reynolds number and the thermophysical properties of the nanofluids affect the value of Nusselt number. It was found outside the recirculation zones, nanoparticles having high thermal conductivity (such as Ag or Cu) have more enhancements on the value of the Nusselt number. However, within the primary and secondary recirculation zones, nanoparticles having low thermal conductivity (such as TiO_2) have better enhancement on heat transfer.

References

- Abu-Mulaweh, H.I., 2003. A review of research on laminar mixed convection flow over backward and forward-facing steps. *Int. J. Thermal Sci.* 42, 897–909.
- Abu-Nada, E., 2006. Entropy generation due to heat and fluid flow in backward facing step flow with various expansion ratios. *Int. J. Energy* 3 (4), 419–435.
- Abu-Nada, E., Al-Sarkhi, A., Akash, B., Al-Hinti, I., 2007. Heat transfer and fluid flow characteristics of separated flows encountered in a backward facing step under the effect of suction and blowing. *ASME J. Heat Transfer*, in press, doi:10.1115/1.2759973.
- Anderson Jr., J.D., 1995. *Computational Fluid Dynamics: The Basics with Applications*. McGraw Hill, New York.
- Armaly, B.F., Durst, F., Pereira, J.C.F., Schönung, B., 1983. Experimental and theoretical investigation of backward-facing step flow. *J. Fluid Mech.* 127, 473–496.
- Brinkman, H.C., 1952. The viscosity of concentrated suspensions and solutions. *J. Chem. Phys.* 20, 571–581.
- Choi, S.U.S., 1995. Enhancing thermal conductivity of fluids with nanoparticles. In: Siginer D.A., Wang H.P. (Ed.), *Developments and Applications of Non-Newtonian Flows*, FED-Vol. 231/MD-Vol. 66 ASME, New York, 99–105.
- Daungthongsuk, W., Wongwises, S., 2007. A critical review of convective heat transfer nanofluids. *Renew. Sust. Energ. Rev.* 11, 797–817.
- Gartling, D.K., 1990. A test problem for outflow boundary condition–flow over a backward facing step. *Int. J. Num. Methods Fluids* 11, 953–967.
- Khanafer, K., Vafai, K., Lightstone, M., 2003. Buoyancy-driven heat transfer enhancement in a two-dimensional enclosure utilizing nanofluids. *Int. J. Heat Mass Transfer* 46, 3639–3653.
- Kim, J., Moin, P., 1985. Application of a fractional-step method to incompressible Navier-Stokes equations. *J. Comput. Phys.* 59, 308–323.

Li, A., Armaly, B.F., 2002. Laminar mixed convection adjacent to three-dimensional backward-facing step. *ASME J. Heat Transfer* 124, 209–213.

Nie, J.H., Armaly, B.F., 2003. Three-dimensional flow adjacent to backward facing step. *ASME J. Heat Transfer* 125, 422–428.

Patankar, S.V., 1980. *Numerical Heat Transfer and Fluid Flow*. Hemisphere Publishing Corporation, Taylor and Francis Group, New York.

Pepper, D.W., Burton, K.L., Bruenckner, F.P., 1992. Numerical simulation of laminar flow with heat transfer over a backward facing step. In: *Benchmark Problems for Heat Transfer Codes ASME 1992, HTD-Vol. 222*, 21–26.

Shukla, R.K., Dhir, V.K., 2005. Study of the effect of thermal conductivity of nanofluids. In: *ASME International Mechanical Engineering Congress and Exposition*, Orlando, FL, USA.

Thangam, S., Knight, D., 1989. Effect of step height on the separated flow past a backward facing step. *Phys. Fluids* 1 (3), 604–606.

Trisaksri, V., Wongwises, S., 2007. Critical review of heat transfer characteristics of nanofluids. *Renew. Sust. Energ. Rev.* 11, 512–523.

Tylli, N., Kaiktsis, L., Ineichen, B., 2002. Sidewall effects in flow over a backward-facing step: Experiments and numerical solutions. *Phys. Fluids* 14 (11), 3835–3845.

Versteeg, H.K., Malalasekera, W., 1995. *An Introduction to Computational Fluid Dynamics: The Finite Volume Method*. John Wiley and Sons Inc, New York.

Vratis, G.C., Outgen, V., Sanchez, J., 1992. Heat transfer over a backward-facing step: Solutions to a benchmark. In: *Benchmark Problems for Heat Transfer Codes ASME 1992, HTD-Vol. 222*, 27–34.

Wang, X-Q., Mujumdar, A.S., 2007. Heat transfer characteristics of nanofluids: a review. *Int. J. Therm. Sci.* 46, 1–19.

Williams, P.T., Baker, A.J., 1997. Numerical simulations of laminar flow over a 3D backward facing step. *Int. J. Num. Methods Fluids* 24, 1159–1183.